JOURNAL OF BIOCHEMICAL SCIENCES
Jul-Dec 2024, VOL. 1, ISSUE 2, pp. 1-7
https://doi.org/10.61577/jbs.2024.100006

RESEAPRO JOURNALS

ORIGINAL ARTICLE

OPEN ACCESS

In-silico strategies for probing fatty acids-based inhibitors from palm Kernel (*Elaeis guineensis*) Oil against Aldo-Keto Reductase 1C3 (AKR1C3)

Martin Msughter Ganyam[1], Emeka Godwin Anaduaka[2], Sule Ola Salawu[3] and Joel Ireoluwa Yinka[1]

[1]Department of Biochemistry, Federal University of Agriculture, Makurdi
[2]Department of Biochemistry, University of Nigeria, Nsukka, Enugu, Nigeria
[3]Department of Biochemistry, Federal University of Technology, Akure, Ondo, Nigeria

ABSTRACT

Aldo-Keto Reductase 1C3 (AKR1C3) is a vital human enzyme involved in the NADPH-dependent reduction of carbonyl groups in various steroids and prostaglandins. Its overexpression is linked to cancers such as breast, endometrial, and prostate. This study investigated the potential effects of fatty acids from Palm Kernel (Elaeis guineensis) oil on AKR1C3 using GC-MS analysis and in-silico methods. We evaluated Gas Chromatography-Mass Spectrometry (GC-MS) data, physicochemical properties, lipophilicity, pharmacokinetics, Lipinski's drug-likeness, and toxicity of the molecules. Molecular docking studies with AKR1C3 were conducted using Autodock Vina software, followed by validation using the MM/GBSA method and stability assessment through 100 ns molecular dynamics (MD) simulations with Desmond software. Findings revealed that 9-Octadecenoic acid (Z)-2-hydroxy-1-(hydroxymethyl) ethyl ester (-8.2 kcal/mol) exhibited superior binding energies compared to the control ligand, 3-phenoxybenzoic acid (-8.1 kcal/mol). MM/GBSA calculations demonstrated favorable binding affinities, and superimposed RSMD (0.878 Å) poses of ligands showed minimal deviation. Two of the complexes were more stable throughout the 100 ns simulation period, and test compounds displayed satisfactory drug-likeness, physicochemical properties, and toxicity profiles. These promising results suggest further in vivo and in vitro exploration of the lead compounds as potential drug candidates targeting AKR1C3 in hormone-dependent cancers.

KEYWORDS

Aldo–Keto Reductase; GC–MS; Molecular Docking and Molecular Dynamics

ARTICLE HISTORY

Received 14 July 2024; Revised 8 August 2024; Accepted 17 September 2024

Introduction

Aldo–keto reductase 1C3 (AKR1C3) is a human aldo–keto reductase enzyme that catalyses the NADPH-dependent reduction of carbonyl moieties on a variety of steroids and prostaglandins synthesis [1]. Over-expression of AKR1C3 has been implicated in several hormone-dependent malignancies, including breast, endometrial, and prostate cancers, with higher expression levels correlating to increased disease aggressiveness and poor patient prognosis [2-5].

Research on AKR1C3 inhibitors has led to the development of various compounds, such as cyclopentane derivatives, hormone analogues, natural products, non-steroidal anti-inflammatory drug (NSAID) analogues, metal complexes, and sulfonylureas [6]. Despite these efforts, no specific AKR1C3 inhibitor has been successfully commercialized. Current inhibitors face limitations, such as non-specificity and adverse effects associated with long-term use, particularly in the case of NSAIDs [7,8].

Given these challenges, traditional herbs have gained attention as potential alternative sources of AKR1C3 inhibitors due to their natural, eco-friendly nature and potential for fewer adverse effects [9]. The two common varieties of palm kernel oil in Nigeria, *Elaeis guineensis* (virenscens 'Ojukwu' and nigrescens), have been used in traditional medicine [10]. The oil contains unsaturated fatty acids that can be metabolized in the human body to produce important prostaglandins [11].

In this study, we utilized gas chromatography-mass spectrometry (GC–MS) to identify and analyze the fatty acids in palm kernel oil extract. This analytical technique enables the detection of a wide range of compounds, including those found in medicinal plants [12]. Furthermore, we employed computer-aided tools (molecular docking and molecular dynamics) to investigate the potential inhibitory effects and mechanism of these fatty acids on AKR1C3 [13,14]. In-silico techniques provide insight into drug-receptor interactions and allow for the prediction of drug candidate binding to target proteins.

By combining these analytical and computational methods, our research aims to explore the potential of fatty acids in palm kernel oil as natural inhibitors for AKR1C3. The results may contribute to the development of alternative and therapeutic options for hormone-dependent malignancies targeting AKR1C3.

Materials and Methods

Materials

Palm kernel fruits were collected from Gbajimba village, Benue State, and identified by a plant taxonomist from the Department of Botany, Federal University of Agriculture, Makurdi, Benue State, Nigeria.

***Correspondence:** Martin Msughter Ganyam, Department of Biochemistry, Federal University of Agriculture, Makurdi, e-mail: ganyamm@yahoo.com

Methods

Palm kernel preparation

Palm kernel fruits were boiled for 2 hours at 100°C, air-dried for 48 hours, de-shelled, and homogenized by pounding for 30 minutes.

Palm kernel oil extraction

Palm kernel oil was extracted using a Soxhlet extractor with n-hexane as the solvent following the method of [15]. Briefly, 25g of crushed palm kernel was loaded into the Soxhlet extractor, and the extraction was carried out for 6 hours. After extraction, n-hexane was evaporated using a water bath, yielding 50ml of palm kernel oil.

GC-MS and phytochemical analysis

The GC-MS analysis was performed using Shimadzu GC-MS-QP2010 PLUS under specified conditions: injector temperature at 250°C, oven temperature at 60°C, ion source temperature at 200°C, interface temperature at 250°C, pressure at 100.2 KPa, column flow at -1.61 ml/min, purge flow at 5.6 ml/min, and total flow rate at 39.4 ml/min. Manual injection of the sample was done at a split ratio of 20:0, and the total running time was 11 minutes. The National Institute of Standard and Technology (NIST) library database was used for mass spectrum interpretation.

ADME and protox prediction

SwissADME (http://www.swissadme.ch/index.php) was used to profile the physicochemical, lipophilicity, pharmacokinetics, and Lipinski's drug-likeness of 46 ligands. Toxicity assessment was performed on Protox (http://tox.charite.de/protoxII). All the ligands were compared to the control ligand 3-phenoxybenzoic acid and ranked based on their ADME and toxicity profiles to find the top drug-like candidates.

Protein and ligand preparation

The crystal structure of Escherichia Aldo-Keto Reductase 1C3 (PDB 3UWE) is similar to the other structures in the aldo-keto reductase family [16]. 3UWE was obtained from Protein Data Bank (PDB) database (https://www.rcsb.org/structure/3uwe) and refined using Discovery Studio (2016) [17] Visualizer, following a refinement protocol that included addition of polar hydrogens, assigning AD4 type atoms, and computing Gasteiger charges. The protein-ligand binding pockets were obtained from literature [18]. Ligands were obtained in 'sdf' format from Pub Chem (www.pubchem.ncbi.nlm.nih.gov) open chemistry database and optimized using Avogadro2 software (https://two.avogadro.cc/). The optimization involved an energy minimization step with MMFF94 (Merck Molecular Force Field 94) force field, 4 steep per update, and the steepest decent algorithm. This was followed by saving the ligands as 'pdb' files for further assessment and molecular docking.

Molecular docking

Auto Dock Vina version 1.5.7 was used to perform docking, and binding affinities of the ligands were calculated [19]. The grid box for the active site ASP50 was set at x = 6.431, y = 1.774, and z = 11.775, using Gauss View 5.0 [20] to get the receptor coordinates with dimensions of 24 × 24 × 24Å for x, y, and z, respectively. The protein and ligands were prepared in 'pdbqt' format for docking using command lines and the value for exhaustiveness was 8 with a default energy range of 3.0kcal/mol.

MMGBSA calculations

Binding free energies were calculated using MM-GBSA, VSGB 2.0 implicit solvation model, and OPLS-2005 via Prime [21]. The binding free energy was calculated using the equation:

$$\Delta Gbind = Gcomplex - Gprotein - Gligand \quad (1)$$

Where G complex, Gprotein, and Gligand represent the free binding energy of the protein-ligand complex, protein, and ligand, respectively.

Post-docking analysis

Protein-ligand complexes were analyzed using Ligplot+ (version 2.2.5) [22] to identify potential hydrogen bond interactions and possibilities for non-covalent bond formation [23]. The Superposition module from Maestro was employed to overlay the re-docked co-crystallized ligand with the ligands itself, to confirm the validity of the docking protocol implemented [24].

Molecular dynamic simulation analysis

The stability of the best-docked complex was evaluated through a 100 ns MD simulation using Desmond software [25]. The system was prepared using a protein preparation wizard and refined by PROKA pH. The simulation environment model was created using the TIP3P solvation model, and an orthorhombic box of dimensions 10x10x10 Å was used. Na+ and Cl—ions were added to neutralize the system. The entire system was optimized using the OPLS3e force field [26-28].

The simulation time was set at 100 ns with recording intervals specified as 100.00ps for trajectory and 1.2 for energy. This would result in approximately 1000 frames. The simulation was run in the NPT ensemble class, with a temperature of 300.0K and pressure of 1.01325 bar. Before the simulation, the model system was relaxed using the default relaxation protocol. RESPA integrator parameters include a Time step (fs): bonded: 2.0 near:2.0 far: 6.0. For the ensemble, the Nose-Hoover chain thermostat method was chosen with a relaxation time of 1.0ps. For interactions, the Coulombic method was used with a short-range cutoff method. The cutoff radius was set at 9.0 Å. Maestro Simulation interaction diagram module was used to calculate the following values: Root Mean Square Deviation (RMSD) was calculated by aligning with the protein RSMD, root-mean-square fluctuation (RMSF), protein-ligand interactions, radius of gyration (rGyr), Solvent Accessible Surface Area (SASA), and Polar Surface Area (PSA). Also, the maestro simulation interaction diagram module was used to plot the corresponding graphs.

Results

GC–MS results of palm kernel oil extract

Forty-six (46) compounds were identified in the GCMS analysis of the crude extract with their retention time as shown on the chromatogram (Table S1). From the GC–MS chromatogram below, the two promising compounds Dodecanoic acid ethyl ester and 9-Octadecenoic acid (Z)-2-hydroxy-1-(hydroxymethyl) ethyl ester had a retention time of 19.634 and39.169 respectively (Figure 1).

ADME and toxicity profiling

We initially screened a library of 46 compounds based on their ADME and toxicity profiles. Twelve (12) candidates with the highest drug-like potential were identified. These compounds

https://doi.org/10.61577/jbs.2024.100006

were expected to reach the site of action and produce favorable biological activity. None of these compounds violated Lipinski's rules, and all were predicted to have high intestinal absorption, except for p-Mentha-1,5,8-triene (PubChem CID: 527424), 1,4-Cyclohexadiene-3-ethenyl-1,2-dimethyl- (PubChem CID: 576908), and 1H-Indene-1-methylene- (PubChem CID: 75581). However, most of the compounds penetrated the blood-brain barrier (BBB). (Table S2).

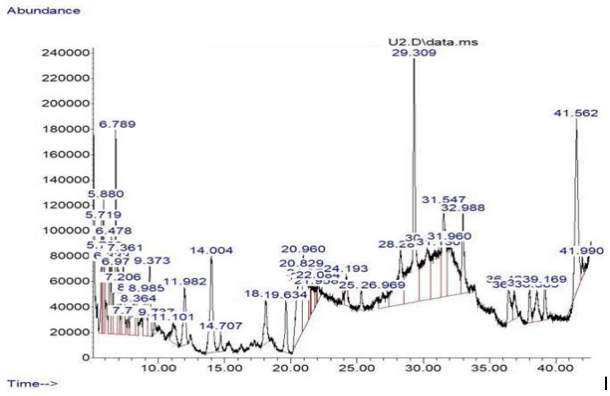

Figure 1. GC–MS Chromatogram of Palm Kernel Oil Extract.

Table 1. Impact of metformin on Superoxide Dismutase.

Eleven (11) of the top twelve (12) compounds exhibited no potential for toxicity, except for 1-Ethyl-2-methylpropylisopropylphosphonofluoridate (PubChem CID: 581214), which fell under toxicity class 1. The LD50 values ranged from 10000 mg/kg to 1 mg/kg (Table S3). 11 compounds were therefore selected for molecular docking.

Molecular docking

The docking score of the 11 compounds ranged from -8.1kcal/mol to -6.2kcal/mol with the control ligand, 3-phenoxybenzoic acid (PubChem CID: 19539), exhibiting a binding energy of -8.1 kcal/mol. Dodecanoic acid ethyl ester (PubChem CID: 7800) and 9-Octadecenoic acid (Z)-2-hydroxy-1(hydroxymethyl) ethyl ester (PubChem CID:5319879) displayed the highest binding energies of -8.3 kcal/mol and -8.2 kcal/mol, respectively. In contrast, 2-Hexenal- (E)- (PubChem CID:5281168) showed the lowest binding energy value of -4.5 kcal/mol. Other ligands had binding energies ranging from 5.5 kcal/mol to -6.9 kcal/mol (Table 1). The highest docking score of the 2 compounds with the control were revalidated using MMGBSA protocol revealed a binding affinity of -61.30 kcal/mol (Dodecanoic acid ethyl ester), -59.44 kcal/mol (9-Octadecenoic acid (Z)-2-hydroxy-1(hydroxymethyl) ethyl ester and -76.63 kcal/mol (3-phenoxybenzoic acid (control) (Table 2).

Ligands	Binding energy (Kcal/mol)	Hydrogen Bonds and Distance (Å)	Interacting amino acids
p-Mentha-1,5,8-triene	-6.7	Tyr55 (2.89) Ser217(3.10)	Tyr216, Leu268, Gly222, Lys270, Phe306
1-o-Tolylprop-2-en-1-	-6.4	Tyr55 (3.08) His117(3.09)	Tyr24, Trp227, Leu54
1,4-Cyclohexadiene,3-ethenyl-1,2-dimethyl-	-6.4	None	Tyr24, Tyr55, His117, Tyr216, Phe306
1H-Indene- 1-methylene-	-6.6	None	Tyr24, Tyr216, Trp227, Phe306
Phenol-2-ethyl-4-methyl-	-6.2	Tyr55(3.08) His117(3.09)	Tyr24, Leu54, Tyr216, Trp227, Phe306
Propofol	-6.9	Tyr55(2.83)	His117, Tyr216, Leu268, Phe306, Gly22
Dodecanoic acid ethyl ester	-8.3	Tyr55(2.99)	Met120, Tyr317, Pro318, Phe311, Tyr319, Leu268, ser217, tyr216, Asn167, Phe306
Dodecanoic acid	-7	Leu219(3.19) Ala218 (2.89)	Trp227, Phe306, Phe311, Tyr24, Tyr55, Lys270, Leu268, Ser217
Dodecanoic acid-2-butoxyethyl ester	-7.9	Ser217(3.23) Lys270(2.96)	Met120, Phe311, Gln222, Leu219, Phe306, Tyr216, His117, Asn167, Ser118
Ethyl trans-3-isopropyl-2-oxiranecarboxylate	-5.5	Ser217(3.21) Gln222 (2.19)	Tyr216, Ser221, Leu268, Lys270
2-Ethylbutyric acid-2-hexyl ester	-6.7	Tyr55(2.99)	Tyr24, His117, Tyr216, Phe306, Phe311
9-Octadecenoic acid (Z)-2-hydroxy-1 (hydroxymethyl) ethyl ester	-8.2	Lys270(2.79, 3.08)	Met120, Leu122, Phe311, Ser217, Tyr216, Leu122
3-phenoxy benzoic acid(control)	-8.l	Tyr319 (3.02), Asn167 (3.06), Tyr216 (2.91)	His117, Tyr55, Phe306, Met120, Phe311

https://doi.org/10.61577/jbs.2024.100006

RESEAPRO JOURNALS

Revalidating docking scores using MMGBSA

Additionally, the Prime MMGBSA module analyzed the binding energy calculation of selected top two compounds based on their binding affinity towards the active site binding pocket of the target molecule. MMGBSA score of the lead molecule Dodecanoic acid ethyl ester was -61.30, whereas the second lead molecule 9-Octadecenoic acid (Z)- 2-hydroxy-1 (hydroxymethyl) ethyl ester showed a slightly lower MMGBSA score of-59.44 (Table 2).

Table 2. Rescoring docking of top two ligands and control using MMGBSA

Ligands	Docking Score (kcal/mol)	MMGBSA (kcal/mol)
3-phenoxy benzoic acid (Control)	-8.1	-76.63
Dodecanoic acid ethyl ester	-8.3	-61.30
9-Octadecenoic acid (Z)- 2-hydroxy-1 (hydroxymethyl) ethyl ester	-8.2	-59.44

Post-docking analysis of the control ligand using LigPlot+ (version 2.2) showed that the complex formed by 3-phenoxybenzoic acid with AKR1C3 revealed three hydrogen bonds interaction with Asn167 (3.06 Å), Tyr216 (2.91 Å), and Tyr319 (3.02 Å) residues (Figure 2, Table 1). In contrast, the Dodecanoic acid ethyl ester complex with AKR1C3 formed one hydrogen bond with Tyr55 (2.99 Å) and hydrophobic interactions with Met120, Pro318, Tyr317, Tyr319, Phe311, Asn167, Tyr216, Ser217, and Leu268 while 9-Octadecenoic acid (Z)-2-hydroxy-1-(hydroxymethyl) ethyl ester formed a complex with AKR1C3, revealing two hydrogen bonds with Lys270 (2.79 Å, 3.08 Å) and 12 hydrophobic interactions (Figure3).

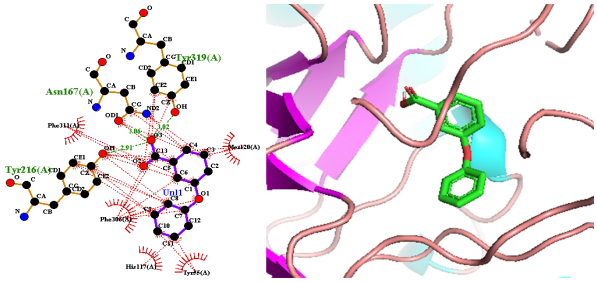

Figure 2. The complex formed between the control ligand (3-phenoxy benzoic acid) and Aldo–Keto Reductase 1C3 (AKR1C3).

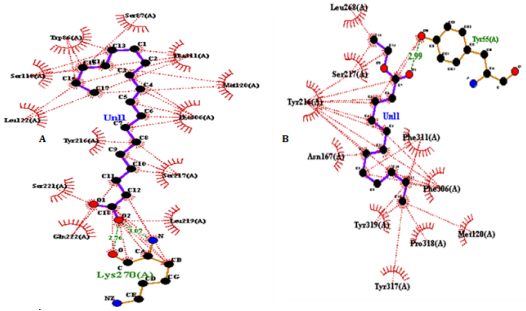

Figure 3. The 2D hydrophobic interaction (red curved lines) and hydrogen bond (green dashed lines) formation between ligands and the amino acid residue of the receptor using LigPlot. A: Dodecanoic acid ethyl ester and B: 9-Octadecenoic acid (Z)-2-hydroxy-1-(hydroxymethyl) ethyl ester.

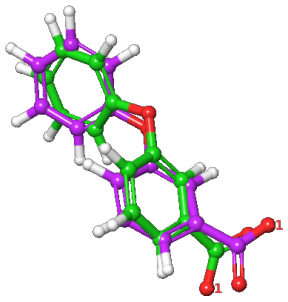

Figure 4. Co-crystallized ligand (Green) extracted and re-docked (purple). Poses superimposed (RSMD: 0.878Å).

Molecular dynamics

Two compounds and controls were subjected to molecular dynamics simulations to predict the stability of the complexes and validate the bonds formed and their corresponding strength. The RMSD measurements were used to evaluate the stability of the docked complexes. The RMSD value of the 3 compounds ranged from 2.2 Å to 2 Å with an average shift of ~1-3 Å (Figure 5-7a). The 9-Octadecenoic acid (Z)-2-hydroxy-1 (hydroxymethyl) ethyl ester complex was stable throughout the simulation except for a minor drift during the 15ns to 20ns timeline. Dodecanoic acid ethyl ester complex was shown to be moderately stable. The complex initially showed moderate drift, but after 45, it became more stable (Figure 6a). 3-phenoxy benzoic acid complex stayed quite consistently stable throughout the analysis, with an average RMSD value of the complex of ~2 Å (Figure 7a).

Minor fluctuations in RMSF were noticed in all three complexes, but no major alterations were observed throughout the experiment. Each complex remains stable (Figure 5-7b). The protein-ligand contact interactions showed that different residues were in contact with the ligand for different durations during the simulation (Figure 5-7c).

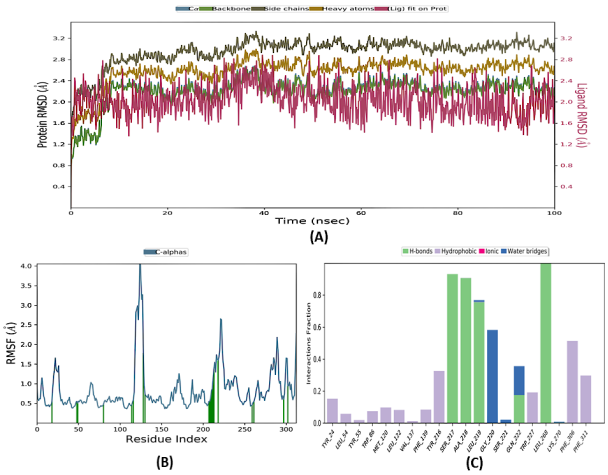

Figure 5. 9-octadecanoic acid (Z) - 2-hydroxy-1-(hydroxymethyl) ethyl ester with Aldo-keto-reductase 1C3 protein: A) RMSD, B) RMSF, C) Protein-Ligand Contacts with interaction fraction: This shows for how long during the simulation timeline the residues were in contact with the ligands. For values ranging from 0-1, 1 means that there was contact 100% of the simulation time and 0 for no contact during the simulation time.

https://doi.org/10.61577/jbs.2024.100006

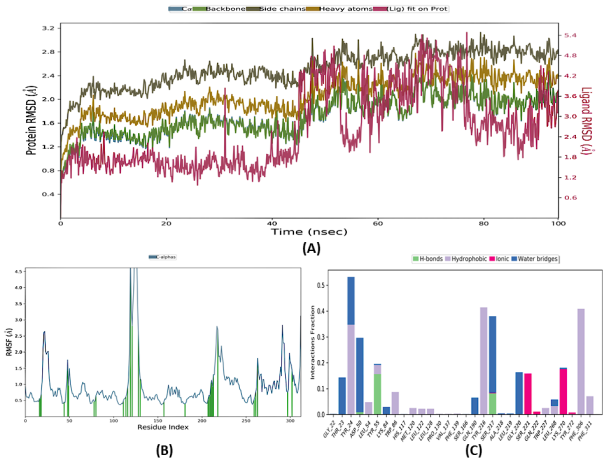

Figure 6. Dodecanoic acid ethyl ester with Aldo-keto-reductase 1C3 protein: A) RMSD, B) RMSF, and C) Protein-Ligand Contacts with Interaction Fraction: These show for how long during the simulation timeline the residues were in contact with the ligands. For Values ranging from 0-1, 1 means that there was contact 100% of the simulation time and 0 for no contact during the simulation time.

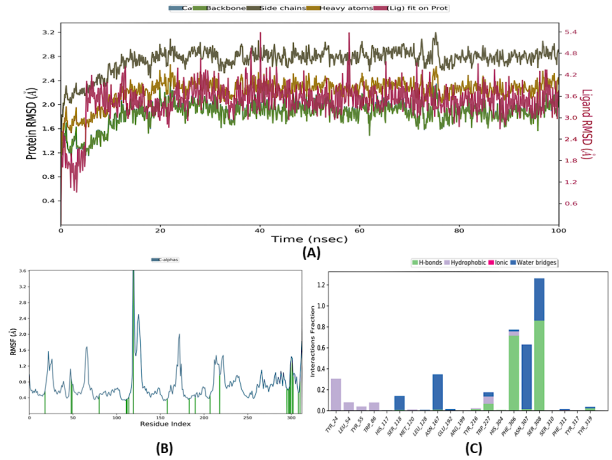

Figure 7. 3-phenoxy benzoic acid with Aldo-keto-reductase 1C3 protein: A) RMSD, B) RMSF, and C) Protein-Ligand Contacts with Interaction Fraction: These shows for how long during the simulation timeline the residues were in contact with the ligands. For Values ranging from 0-1, 1 means that there was contact 100% of the simulation time and 0 for no contact during the simulation time.

Protein-ligand interaction analysis was also performed: It was discovered that the ligand 9-Octadecenoic acid (Z)-2-hydroxy-1 (hydroxymethyl) ethyl ester interacted with 20 amino acids of the protein Aldo keto-reductase 1C3 across the simulation period, including Tyr24 (0.15Å), Leu54 (0.05Å), Tyr55 (0.02Å), and Trp86 (0.075Å). Met120(0.1Å), Leu122(0.075Å), Val137 (0.02Å), Phe139 (0.075Å), Tyr216(0.35), Ser217(0.9Å), Ala218 (0.875Å), Leu219 (0.75Å), Gly220 (0.6Å), Ser221 (0.03Å), Gln222(0.4Å), Trp227 (0.2Å), Leu 268 (1.0Å), Lys270(0.02Å), Phe306 (0.5Å) andPhe311 (0.3Å); Dodecanoic acid ethyl ester interacted with 30 amino acids of the protein Aldo keto-reductase 1C3 which are Gly22 (0.01Å), Thr23 (0.13Å), Tyr24 (0.55Å), Asp50(0.3Å), Leu54 (0.04Å), Tyr55 (0.2Å), Lys84 (0.03Å), Trp86 (0.1Å), His117 (0.01Å), Met120 (0.03Å), Leu122(0.03Å), Leu128(0.03Å),Pro130(0.01Å), Val137(0.01Å), Phe139(0.01Å), Ser166(0.01Å), Gln190 (0.05Å), Tyr216 (0.4Å), Ser217 (0.375Å), Ala218 (0.01Å), Leu219 (0.01Å), Gly220 (0.175Å), Ser221(0.175Å), Gln222 (0.02Å), Trp227 (0.03Å), Leu268 (0.05Å), Lys270 (0.2Å), Tyr272 (0.02Å), Phe306 (0.4Å), Phe311 (0.05Å); 3-phenoxybenzoic acid interacted with 21 amino acids of Aldo-keto-reductase 1C3 protein that includes Tyr24 (0.3Å), Leu54 (0.05Å), Tyr55 (0.02Å), Trp86 (0.05Å), His117 (0.01Å), Ser118 (0.18Å), Met120 (0.01Å), Leu128 (0.01Å), Asn167 (0.4Å), Glu192 (0.02Å), Arg199 (0.01Å). Tyr216 (0.03Å), Trp227 (0.2Å), His304 (0.01Å), Phe306 (0.8Å), Asn307 (0.6Å), Ser308 (1.2Å), Ser310 (0.01Å), Phe311 (0.02Å), Tyr317 0.01Å) and Tyr319 (0.05Å). These interacting residues are all represented as vertical green bars in RMSF graphs, demonstrating their stability under dynamic settings (Figures 5,6 and 7).

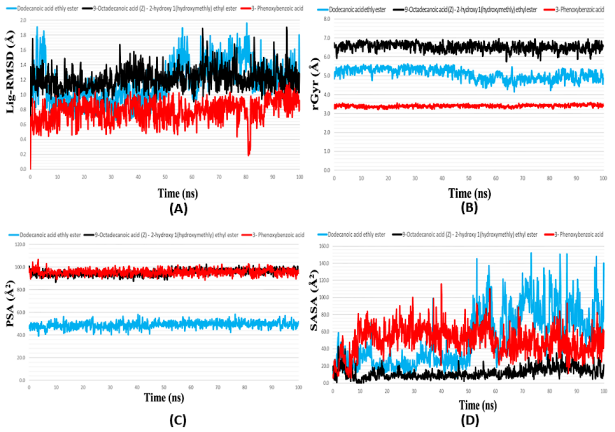

Figure 8. Ligand properties during 100ns MD simulation with Aldo-keto-reductase 1C3 protein: A) Ligand-RMSD, B) The radius of gyration (RGyr), C) Polar Surface Area (PSA) and D) Solvent Accessible Surface Area (SASA).

The radius of gyration is a key parameter of the protein drug complex used to study the folding properties and conformations of the protein drug complexes. A comparatively high radius of gyration value indicates that a protein molecule is packed loosely, while a lower radius indicates a more compact protein structure. A more compact protein indicates that the drug molecule has not significantly interfered with the folding mechanism of the protein. Analysis of the radius of the gyration parameter (Figure 8B) shows all the experimented complexes to be compact, and neither one displayed a greater amount of fluctuation under dynamic conditions. The average RGyr value of 9-Octadecenoic acid (Z)-2-hydroxy-1 (hydroxymethyl) ethyl ester complex, dodecanoic acid ethyl ester complex, and 3-phenoxy benzoic acid complexes were 6.5Å, 5.1 Å and 3.4 Å respectively. Although the 3-phenoxy benzoic acid complex appeared to be compact and tight in the overall MD simulation, the 9-Octadecenoic acid (Z)-2-hydroxy-1 (hydroxymethyl) ethyl ester complex was the most stable.

Protein Aldo keto reductase 1C3 with ligand 9-Octadecenoic acid (Z)-2-hydroxy-1-(hydroxymethyl) ethyl ester complex and protein Aldo-keto-reductase 1C3 with ligand 3-phenoxy benzoic acid complexes showed similar PSA curve throughout the simulation period (Figure 8C). The average PSA for both these complexes was 98 Å2. While for Protein Aldo keto reductase 1C3 with ligand Dodecanoic acid ethyl ester complex, the average PSA was 49Å2.

Solvent Accessible Surface Area analysis (SASA) reveals a better understanding of the protein-drug complexes'

https://doi.org/10.61577/jbs.2024.100006

hydrophobic and hydrophilic behaviour. For SASA (Solvent accessible surface area) the protein Aldo keto reductase 1C3 with ligand Dodecanoic acid ethyl ester complex showed the highest SASA of 150 Å2, while the Protein Aldo keto reductase 1C3 with ligand 9-Octadecenoic acid (Z)-2-hydroxy-1-(hydroxymethyl) ethyl ester complex showed lowest SASA. The protein Aldo-keto-reductase 1C3 with ligand 3-phenoxy benzoic acid complex displayed a moderate value as observed in Figure 8D

The Root Mean Square Deviation (RMSD) analysis is an important step towards measuring the stability of the protein-ligand complex. A stable RMSD indicates that the binding of the protein-drug complex does not cause any significant changes in the structure of the protein.

Ligand RMSD refers to the Root mean square deviation of a ligand with respect to the reference conformation. The Protein Aldo keto reductase 1C3 with Dodecanoic acid ethyl ester complex showed the most fluctuation here with a maximum value of 1.9 Å and minimum of 0.6 Å. The other two complexes of Aldo keto reductase 1C3 with 9-Octadecenoic acid (Z)-2-hydroxy-1 (hydroxymethyl) ethyl ester complex and 3-phenoxy benzoic acid displayed a more compact curve and stability in their ligand-RMSD curve (Figure 8A). For each complex value less than 3Å indicates stability.

Discussion

In this study 46 compounds were identified from GC-MS analysis of palm kernel oil extracts. 11 of these compounds passed various drug-likeness and toxicity tests. Two (2) of the compounds were promising with the highest binding affinity: Dodecanoic acid ethyl ester (-8.3 kcal/mol) (Compound I); 9-Octadecenoic acid (Z)-2-hydroxy-1(hydroxymethyl) ethyl ester (-8.2 kcal/mol) (Compound II). These 2 compounds were subjected to molecular dynamic simulations and showed stable conformations with RMSD values ranging from 2.2 Å to 2 Å. Other MD simulation parameters (RMSF, rGyr, PSA, SAS) were considered, suggesting the complexes' stability as explained in our results.

The first aim of this study was to find an effective inhibitor of AKR1C3 from a natural source. Our choice was palm kernel oil. We deem this to be important because current inhibitors of AKR1C3 are NSAIDs, and studies have shown that long-term usage leads to various systemic toxicity (gastric, renal, and cardiovascular) [7,8]. Secondly, we aimed to suggest a specificity and putative inhibition mechanism from our data.

As stated above, two compounds with high binding affinity were identified and formed stable complexes. To elucidate the inhibitory and specificity mechanism, we had to study the binding sites of AKR1C3. There are 5 compartments: oxyanion site, which is the catalytic site (Asp50, Tyr 55, Lys84, His117); steroid channel (Tyr24, Leu54, Ser129, Trp227); SP1 (Ser118, Asn167, Phe306, Phe311, Tyr319); SP2 (Trp86, Leu122, Ser129, Phe311), and SP3 (Tyr24, Glu192, Ser221, Tyr305) sub-pockets [29,30]. Previous inhibitors [6,30] have been designed to exploit the conserved nature of SP1-3 sub-pockets in AKR1C3 for specificity.

Based on this observation we were able to elucidate that the compounds may competitively inhibit AKR1C3, firstly, because, of strong hydrogen bonds formed during molecular dynamics by the compounds with residues (distance of H bond in Å) in the oxyanion site (catalytic site)–Compound I: Asp50 (0.3Å), Tyr55 (0.2Å), Lys84 (0.03Å) and His117 (0.01Å), Compound II: Tyr55 (0.02Å). Secondly, interaction with residues in the steroid channel Compound I: Tyr24 (0.55Å), Leu54 (0.04Å) and Trp227 (0.03Å), compound II: Tyr24 (0.15Å), Leu54 (0.05Å), and Trp227 (0.2Å). [1] suggested that interactions with residues in the steroid channel guide the substrate for efficient binding at the catalytic site (oxyanion site). We also suggest that specificity is achieved via interactions with SP1-3 residues. Compound I: SP1: Phe306 (0.4Å) and Phe311 (0.05Å), SP2: Trp86 (0.1Å), Leu122 (0.03Å) and Phe311 (0.05Å), SP3: Tyr24 (0.55Å) and Ser221 (0.175Å); Compound II: SP1: Phe306 (0.5Å) and Phe311 (0.3Å). SP2 Trp86 (0.075Å), Leu122 (0.075Å), and Phe311 (0.3Å) and SP3: Tyr24 (0.15Å) and Ser221 (0.03Å)), both compounds seem to exhibit a good specificity as they interacted with same residues in the SPI pocket. These binding mechanisms are also in line with the work of [29] who reported that AKR1C3 possesses a large active site with multiple ligand-binding cavities annotated as the oxyanion site, steroid channel, and sub pockets SP1, SP2, and SP3. [29] further reported that all of the previously characterized inhibitors of AKR1C3 share the common characteristic of an occupied SP1 site, which is lined by residues Phe306, Phe311, Tyr319, Ser118 and Asn167.Dodecanoic acid ethyl ester (Compound I) and 9-Octadecenoic acid (Z)-2-hydroxy-1(hydroxymethyl) ethyl ester (Compound II) are no exception.

Overall, our data suggests that the fatty acid,9-Octadecenoic acid (Z)-2-hydroxy-1(hydroxymethyl) ethyl ester (compound II) present in palm kernel oil may effectively inhibit AKR1C3 with little or no toxicity. However, we were not able to demonstrate exclusive specificity for AKR1C3, also, our extrapolations are based on simulations and there is need for in-vitro and in vivo data to support our claims.

Conclusions

The compound 9-Octadecenoic acid (Z)-2-hydroxy-1-(hydroxymethyl) ethyl ester has been predicted to possess inhibitory potentials for AKR1C3. The rigorous analysis of the MDS data further validated simulated complexes and binding affinity with bonding interactions formed.

Acknowledgements

We acknowledge all those who, in one way or another, contributed to the success of this work. We greatly appreciate all the referenced authors for their intellectual contributions.

Disclosure statement

No potential conflict of interest was reported by the authors.

References

1. MSuzuki-Yamamoto T, Nishizawa M, Fukui M, Okuda-Ashitaka E, Nakajima T, Ito S, et al. cDNA cloning, expression and characterization of human prostaglandin F synthase. FEBS Lett. 1999;462:335-340. https://doi.org/10.1016/S0014-5793(99)01551-8
2. Guise CP, Abbattista MR, Singleton RS, Holford SD, Connolly J, Dachs GU, et al. The bioreductive prodrug PR-104A restores three-dimensional genome access and circumvents hypoxia in solid tumor cells. Cancer Res. 2010;70(4):1573-1584. https://doi.org/10.1158/0008-5472.CAN-09-2740
3. Hofland J, Van Weerden WM, Dits NF, Steenbergen J, Van Leenders GJ, Jenster G, et al. Evidence of limited contributions for intratumoral steroidogenesis in prostate cancer. Cancer Res. 2010; 70(3):1256-1264. https://doi.org/10.1158/0008-5472.CAN-09-2092
4. Lin HK, Steckelbroeck S, Fung KM, Jones AN, Penning TM. Characterization of a monoclonal antibody for human aldo-keto

https://doi.org/10.61577/jbs.2024.100006

reductase AKR1C3 (type 2 3α-hydroxysteroid dehydrogenase/type 5 17β-hydroxysteroid dehydrogenase); immunohistochemical detection in breast and prostate. Steroids. 2004;69(13-14):795-801. https://doi.org/10.1016/j.steroids.2004.09.014
5. Stanbrough M, Bubley GJ, Ross K, Golub TR, Rubin MA, Penning TM, et al. Increased expression of genes converting adrenal androgens to testosterone in androgen-independent prostate cancer. Cancer Res. 2006;66(5):2815-2825. https://doi.org/10.1158/0008-5472.CAN-05-4000
6. Endo S, Oguri H, Segawa J, Kawai M, Hu D, Xia S, et al. Development of novel AKR1C3 inhibitors as new potential treatment for castration-resistant prostate cancer. J Med Chem. 2020;63(18):10396-10411. https://doi.org/10.1021/acs.jmedchem.0c00939
7. Murray MD, Brater DC. Renal toxicity of the nonsteroidal anti-inflammatory drugs. Annu Rev Pharmacol Toxicol. 1993;33(1):435-465. https://doi.org/10.1146/annurev.pa.33.040193.002251
8. Bjorkman D. Nonsteroidal Anti-inflammatory Drug-Associated Toxicity of the Liver, Lower Gastrointestinal Tract, and Esophagus. Am J Med. 1998;105(5):17S-21S. https://doi.org/10.1016/S0002-9343(98)00276-9
9. Sahoo N, Manchikant P. Herbal drug regulation and commercialization: an Indian industry perspective. J Altern Complement Med. 2013;19(12):957–963. https://doi.org/10.1089/acm.2012.0275
10. Stone PB. Elaeis guineensis (African oil palm). CABI Compendium. 2022. https://doi.org/10.1079/fc.20295.20210113788
11. Sehgal S, Sharma V. Palm/palm kernel (Elaeis guineensis). Oilseeds: health attributes and food applications. 2021:145-161. https://doi.org/10.1007/978-981-15-4194-0_6
12. Razack S, Hemanth Kumar K, Nallamuthu I, Naika M, Khanum F. Antioxidant, biomolecule oxidation protective activities of Nardostachys jatamansi DC and its phytochemical analysis by RP-HPLC and GC-MS. Antioxidants. 2015;4(1):185–203. https://doi.org/10.3390/antiox4010185
13. Sliwoski G, Kothiwale S, Meiler J, Lowe EW. Computational methods in drug discovery. Pharmacol Rev. 2014;66(1):334–395. https://doi.org/10.1124/pr.112.007336
14. Lee K, Kim D. In-Silico molecular binding prediction for human drug targets using deep neural multi-task learning. Genes. 2019;10(11):906. https://doi.org/10.3390/genes10110906
15. Redfern J, Kinninmonth M, Burdass D, Verran J. Using soxhlet ethanol extraction to produce and test plant material (essential oils) for their antimicrobial properties. J Microbiol Biol Educ. 2014;15(1):45-46. https://doi.org/10.1128/jmbe.v15i1.656
16. Farber GK, Petsko GA. The evolution of alpha/beta barrel enzymes. Trends Biochem Sci. 1990;15(6):228-234. https://doi.org/10.1016/0968-0004(90)90035-A
17. Biovia D, Berman H, Westbrook J, Feng Z, Gilliland G, Bhat T, et al. Dassault systèmes BIOVIA, Discovery Studio Visualizer, v. 17.2. Dassault Systèmes, San Diego; 2016. J Chem Phys. 2000. https://doi.org/10.12691/jfnr-9-3-3
18. Jackson VJ, Yosaatmadja Y, Flanagan JU, Squire CJ. Structure of AKR1C3 with 3-phenoxybenzoic acid bound. Acta Crystallographica Section F: Structural Biology and Crystallization Communications. 2012;68(4):409-413. https://doi.org/10.1107/S1744309112009049
19. Trott O, Olson AJ. AutoDock Vina: improving the speed and accuracy of docking with a new scoring function, efficient optimization, and multithreading. J Comput Chem. 2010;31(2):455-461. https://doi.org/10.1002/jcc.21334
20. Nielsen AB, Holder AJ. Gauss View 5.0, User's Reference. GAUSSIAN Inc., Pittsburgh; 2008.
21. Lyne PD, Lamb ML, Saeh JC. Accurate prediction of the relative potencies of members of a series of kinase inhibitors using molecular docking and MM-GBSA scoring. J Med Chem. 2006;49(16):4805-4888. https://doi.org/10.1021/jm060522a
22. Wallace AC, Laskowski RA, Thornton JM. LIGPLOT: a program to generate schematic diagrams of protein-ligand interactions. Prot Eng. 1995;8(2):127-134. https://doi.org/10.1093/protein/8.2.127
23. Sharif A, Hossen S, Shaikat MM, Abir AB, Roy PK, Jahan R, et al. Molecular optimization, docking and dynamic simulation study of selective natural aromatic components to block E2-CD81 complex formation in predating protease inhibitor resistant HCV influx. Int J Pharm Res. 2021;13(2):3511-3525.
24. Maestro Schrödinger Release 2020-3: Maestro, Schrödinger, LLC, New York, NY, 2020.
25. Bowers KJ, Chow E, Xu H, Dror RO, Eastwood MP, Gregersen BA, et al. Scalable algorithms for molecular dynamics simulations on commodity clusters. Proceedings of the ACM/IEEE Conference on Supercomputing (SC06); 2006; Tampa, Florida. https://doi.org/10.1145/1188455.1188544
26. Kumar S, Oh JM, Abdelgawad MA, Abourehab MA, Tengli AK, Singh AK, et al. Development of isopropyl-tailed chalcones as a new class of selective mao-b inhibitors for the treatment of parkinson's disorder. ACS Omega. 2023;8(7):6908-6917. https://doi.org/10.1021/acsomega.2c07694
27. Robin TB, Rani NA, Ahmed N, Prome AA, Bappy MNI, Ahmed F. Identification of novel drug targets and screening potential drugs against Cryptococcus gattii: An in silico approach. Inform Med Unlocked. 2023;38:101222. https://doi.org/10.1016/j.imu.2023.101222
28. Zala AR, Rajani DP, Ahmad I, Patel H, Kumari P. Synthesis, characterization, molecular dynamic simulation, and biological assessment of cinnamates linked to imidazole/benzimidazole as a CYP51 inhibitor. J Biomol Struct Dyn. 2023;41(21):11518-11534. https://doi.org/10.1080/07391102.2023.2170918
29. Byrns MC, Jin Y, Penning TM. Inhibitors of type 5 17 β-hydroxysteroid dehydrogenase (AKR1C3): overview and structural insights. J Steroid Biochem Mol Biol. 2011;125:95-104. https://doi.org/10.1016/j.jsbmb.2010.11.004
30. Adeniji AO, Chen M, Penning TM. AKR1C3 as a target in castrate-resistant prostate cancer. J Steroid Biochem Mol Biol. 2020;137(2013):136-149. https://doi.org/10.1016/j.jsbmb.2013.05.012

https://doi.org/10.61577/jbs.2024.100006